

# Graded-Index Polymer Optical Fiber With High Temperature and High Humidity Stability

Takaaki Ishigure, *Member, IEEE*, Masataka Sato, Atsushi Kondo, Yasuyuki Tsukimori, and Yasuhiro Koike, *Member, IEEE*

**Abstract**—It was clarified for the first time that the slight attenuation increment observed in the previous poly methyl methacrylate (PMMA)-dopant system graded-index polymer optical fiber (GI POF) we reported originated in the excess scattering loss induced by the aggregation of absorbed water into the POF. Although the PMMA material generally absorbs two weight% of water at maximum, the low attenuation of the conventional step-index (SI) POF whose core material is PMMA can be maintained at 70 °C, 80% relative humidity (RH) atmosphere because the absorbed water might be homogeneously dispersed without any aggregation in the core of POF. On the other hand, addition of dopant material having higher refractive index than that of PMMA is required to form the refractive index distribution in the GI POF, which decreases the amount of water absorption into polymer, because the dopant material is more hydrophobic than PMMA. Therefore, in spite of the small amount of absorbed water such as 0.5 wt.%, the absorbed water molecules can not be uniformly dispersed but must be aggregated to form heterogeneities in the refractive index of the polymer matrix. It was clarified that a dopant material that is as hydrophilic as PMMA was required to maintain the attenuation of the PMMA-dopant system GI POF under high temperature and high humidity atmosphere, and such a suitable dopant system GI POF was proposed.

**Index Terms**—Dopant, glass transition temperature, humidity resistance, refractive index, temperature resistance, water absorption.

## I. INTRODUCTION

GROWING research interests are focused on the high-speed telecommunications and data communications networks with increasing demand for access to the Internet even from home. In order to transmit a large volume of data such as those of motion pictures, a data rate of several hundreds megabits per second (Mb/s) is required [1]. With increasing demand for high-speed information transmission, recent interests are focused on gigabit-order data transmission such as the gigabit Ethernet system. Therefore, it is desirable to introduce optical fiber networks even to the premises area for covering more than 500–1000 Mb/s data.

We have proposed a large-core, high-bandwidth graded-index (GI) polymer optical fiber (POF) as the physical layer of a short-distance high data rate network [2], [3]. In the GI POF, as the quadratic refractive index profile is formed by the concentra-

tion distribution of the dopant, there was concern that the refractive index profile degraded at a higher temperature than the glass transition temperature ( $T_g$ ) of polymer. When the dopant molecules are added to the polymer matrix, the  $T_g$  is generally lowered due to the plasticization effect. Therefore, the  $T_g$  at the core region of a GI POF is lowered compared with that of PMMA homopolymer. In order to develop a GI POF having high thermal stability, we focused on a  $T_g$  decrease depending on the kinds and concentration of dopant. It was experimentally confirmed that the refractive index profile of the PMMA based GI POF was maintained for more than 5000 h at 85 °C [4], [5] by selecting a suitable dopant which can maintain the high  $T_g$  of PMMA even after doping.

In this paper, not only the thermal stability of the refractive index profile but also the attenuation stability under high temperature and high humidity atmosphere was investigated. We clarified the required characteristics for the dopant in order to maintain the low attenuation of the PMMA based GI POF even at high temperature and high humidity.

## II. THERMAL STABILITY TEST OF PMMA BASED GI POF

### A. PMMA-Dopant System Graded Index Polymer Optical Fiber

The GI POF was prepared by the interfacial-gel polymerization technique which we have proposed [2]. The refractive index profile of the GI POF is formed by the concentration distribution of the dopant which has a higher refractive index than that of the polymer matrix. In the interfacial-gel polymerization process, the GI preform rod that has large diameter such as 20–30 mm was prepared at first. Subsequently, the GI POF was obtained by the heat drawing of the preform at 250 °C. A detailed fabrication procedure is described in elsewhere [3]. Table I shows the dopant candidates for the PMMA based GI POF.

### B. Thermal Stability Test

The thermal stability of the attenuation of the GI POFs doped with several kinds and concentrations of dopant was investigated. The measurement setup is schematically shown in Fig. 1. An InGaAsP laser diode whose emitting wavelength was 655-nm was used as the light source, and the optical output power from a 10-m length GI POF was detected by the optical power meter. On the other hand, a tungsten lamp was also used when the wavelength dependence of the attenuation change caused by aging was measured, and the optical output power was detected using an optical spectrum analyzer. The thermal stability of the attenuation was investigated by continuously

Manuscript received December 28, 2001; revised August 8, 2002.

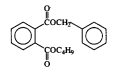
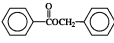
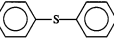
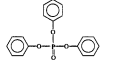
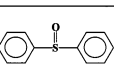
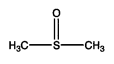
T. Ishigure, A. Kondo, and Y. Koike are with the Faculty of Science and Technology, Keio University, Yokohama 223–8522, Japan, and also with the Japan Science and Technology Corporation, ERATO, Kawasaki 212-0054, Japan.

M. Sato is with the Fuji Photo Film Company, Ltd., Shizuoka, Japan.

Y. Tsukimori is with the Asahi-Kasei Corporation, Kawasaki, Japan.

Digital Object Identifier 10.1109/JLT.2002.804028

TABLE I  
DOPANT MATERIALS USED AND THEIR PHYSICAL PROPERTIES

Monomer and dopant used	Chemical Formula	Molecular Weight (g/mol)	Molecular Volume ( $\text{\AA}^3$ )	Solubility Parameter ( $(\text{cal}/\text{cm}^3)^{1/2}$ )	Refractive index
benzyl n-butyl phthalate (BBP)		312.4	467.5	9.504	1.540
benzyl benzoate (BEN)		212.3	314.6	9.641	1.568
Diphenyl sulfide (DPS)		186.3	277.8	9.431	1.633
triphenyl phosphate (TPP)		326.3	449.2	9.42	1.563
Diphenyl sulfoxide (DPSO)		202.3	286.9	11.95	1.606
Dimethyl Sulfoxide (DMSO)		78.13	117.88	12.0	1.4790

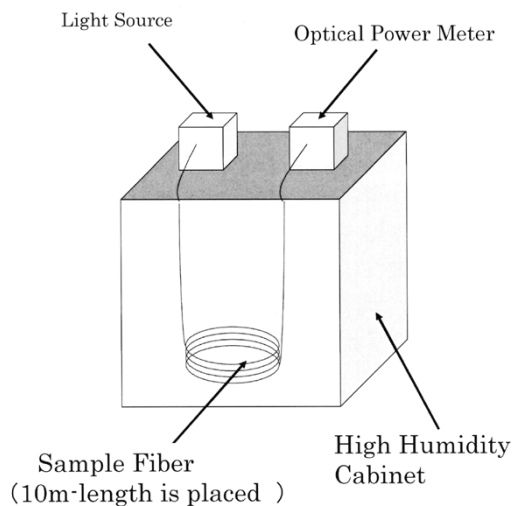


Fig. 1. Measurement apparatus for the high temperature and high humidity resistance of the GI POF.

measuring the output power change during aging. Since the output power from the GI POF is very sensitive to the coupling conditions between the light source and fiber and the fiber and detector, both coupling conditions were fixed during the aging.

### III. RESULTS AND DISCUSSION

#### A. Thermal Stability in the Attenuation of the PMMA Based GI POF

The attenuation increment spectra of the 20-wt.% DPS doped GI POF after 1 and 44 h aging at 70 °C, 80% RH are shown in Fig. 2. It is obvious that a significant attenuation increment is observed after aging. Furthermore, it is noteworthy that large absorption peaks are observed at 750-nm and 840-nm wavelengths, while the wavelength dependence in the attenuation in-

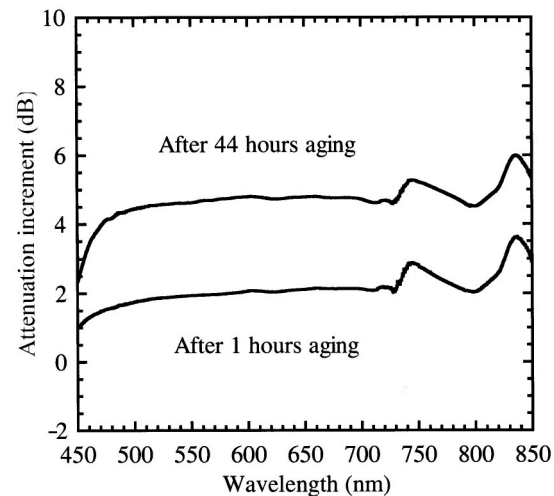


Fig. 2. Wavelength dependence of the attenuation increment of 20 wt.% DPS doped GI POF at 70 °C, 80% RH

crement from 500 nm to 700 nm is small. From the result shown in Fig. 2, the origin of the attenuation increase is discussed as follows:

The peak observed at 750-nm wavelength can be explained by the absorption of oxygen-hydrogen stretching vibration in water molecule absorbed in the GI POF during aging. It is already shown by the Morse potential energy theory [6] that the 4-th overtone absorption of the O-H stretching vibration is located at 750-nm. On the other hand, wavelength independent attenuation increment is difficult to explain by the excess absorption loss such as the overtone of oxygen-hydrogen stretching vibration in the water molecule.

In order to clarify the effect of high humidity on the attenuation spectrum, first, the stability of the attenuation at 70 °C (with low humidity) was measured and compared with the results shown in Fig. 2. The result of the attenuation increment after aging at 70 °C is shown in Fig. 3. Although the wavelength independent attenuation increment is still observed, the amount of increment in Fig. 3 is smaller than that after aging at 70 °C, 80% R.H. shown in Fig. 2. It should be noted that the attenuations around 750- and 840-nm wavelengths actually decrease after aging. This is because the absorption loss due to the O-H bonding decreases during aging, since the water molecules that were absorbed into the GI POF in advance of aging vaporized during aging at 70 °C. Since the PMMA which is the polymer matrix of the GI POF, absorbs approximately 2% of water at maximum, it is possible that some amount of water molecules was absorbed into the GI POF in advance of the aging test. However, as the absorbed water in the GI POF was vaporized during the aging at 70 °C (and low humidity), the optical losses at 750- and 840-nm wavelengths, which were affected by the O-H stretching vibration absorption, decreased.

Although a slight amount of the attenuation increment independent of the wavelength is observed also in Fig. 3, the attenuation increment after 48 h aging at 70 °C (and low humidity) is small compared to that after 44 h aging at 70 °C, 80% R. H. shown in Fig. 2. Therefore, both wavelength dependent and independent attenuation increments shown in Fig. 2 are mainly caused by the high humidity.

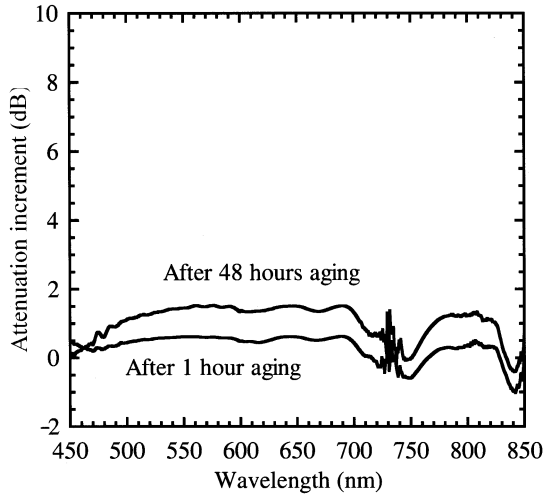


Fig. 3. Wavelength dependence of the attenuation increment of 20 wt.% DPS doped GI POF at 70 °C.

In order to maintain the low attenuation of the GI POF at high temperature, it was found that the numerical aperture and heat drawing condition of the fiber were important issues[7]. By optimizing the fabrication conditions, no attenuation increment was observed during aging at 70 °C. Details of these fabrication conditions and the results of the thermal stability studies were described in elsewhere [7]. Therefore, an excess scattering loss caused by the large heterogeneous structures that were formed by the aggregated water molecules absorbed into the polymer may be one of the candidates for the origin of the attenuation increase shown in Fig. 2.

### B. Excess Scattering Loss

In order to investigate the scattering loss increment after aging at high temperature and high humidity, 20-mm diameter PMMA rod samples doped with the dopants shown in Table I were prepared. The dopant concentration is the same as that in the core center of the GI POF.

For measuring the light scattering loss and investigating the heterogeneities inside the PMMA rod, polarized ( $Vv$ ) and depolarized ( $Hv$ ) light scattering intensities from a He-Ne laser (633 nm-wavelength) were measured against the scattering angle  $\theta$ . The measurement method is described as follows: the PMMA rod was placed vertically at the center of the goniometer, a He-Ne laser beam was injected from the side, and the scattered light from the center region of the rod was detected. The  $Vv$  and  $Hv$  light scattering intensities were measured, the details of which were described in our previous papers [8], [9]. To more quantitatively investigate the heterogeneities in the aged PMMA rod and to estimate the effect of scattering loss on the total attenuation of the GI POF, the scattering intensity measurement results were analyzed by the following procedure.

In randomly oriented polymer samples, the isotropic part  $Vv^{iso}$  of the  $Vv$  is given by (1) [8], [9].

$$Vv^{iso} = Vv - \left(\frac{4}{3}\right)Hv. \quad (1)$$

Therefore, the observed  $Vv$  scattering was divided into three terms,  $Vv_1^{iso}$ ,  $Vv_2^{iso}$ , and  $(4/3)Hv$ , as follows:

$$Vv = (Vv_1^{iso} + Vv_2^{iso}) + \left(\frac{4}{3}\right)Hv \quad (2)$$

where the  $Vv_1^{iso}$  denotes the isotropic background scattering independent of the scattering angle  $\theta$  and the  $Vv_2^{iso}$  is the isotropic scattering which depends on  $\theta$  due to the large sized heterogeneities. Finally, the total scattering loss  $\alpha_t$  (dB/km) is obtained by (3), shown at the bottom of the page, where  $\alpha_t$  is divided into three terms  $\alpha_1^{iso}$ ,  $\alpha_2^{iso}$ , and  $\alpha^{aniso}$  i.e.,

$$\alpha_t = \alpha_1^{iso} + \alpha_2^{iso} + \alpha^{aniso} \quad (4)$$

where  $\alpha_1^{iso}$  is the isotropic scattering loss from  $Vv_1^{iso}$  with no angular dependence,  $\alpha_2^{iso}$  is the isotropic scattering loss from  $Vv_2^{iso}$  due to large-sized heterogeneities, and  $\alpha^{aniso}$  is the anisotropic scattering from  $Hv$ .

Since the angular independence of  $Vv$  indicated the random orientation, Debye's theory[10] written as (5) may be adopted

$$Vv_2^{iso} = \frac{4\langle\eta^2\rangle\pi^3}{\lambda_0^4} \int_0^\infty \frac{\sin(\nu s r)}{\nu s r} r^2 \gamma(\mathbf{r}) dr \quad (5)$$

where

$$\nu = \frac{2\pi n}{\lambda_0} \quad (6)$$

and

$$s = 2 \sin\left(\frac{\theta}{2}\right). \quad (7)$$

Here,  $\langle\eta^2\rangle$  denotes the mean-square average of the fluctuations of all dielectric constants,  $\lambda_0$  is the wavelength of light in vacuum and  $n$  is the refractive index of the sample.  $\gamma(\mathbf{r})$  refers to the correlation function defined by

$$\gamma(\mathbf{r}) = \frac{\langle\eta(\mathbf{r}_i) \cdot \eta(\mathbf{r}_j)\rangle_r}{\langle\eta^2\rangle} \quad (8)$$

where  $\eta(\mathbf{r}_i)$  and  $\eta(\mathbf{r}_j)$  are the fluctuations of the dielectric constant at  $i$  and  $j$  positions that are a distance  $r$  apart. In this paper, the correlation function  $\gamma(\mathbf{r})$  is assumed to be approximated by (9) as suggested by Debye *et al.* [10]

$$\gamma(r) = \exp\left(-\frac{r}{a}\right) \quad (9)$$

where  $a$  is called the correlation length and is a measure of the size of the heterogeneities. Substituting (9) into (5) gives

$$Vv_2^{iso} = \frac{8\pi^3\langle\eta^2\rangle a^3}{\lambda_0^4(1 + \nu^2 s^2 a^2)^2}. \quad (10)$$

$$\alpha_t = 1.346 \times 10^6 \int_0^\pi \left\{ (1 + \cos^2 \theta) (Vv_1^{iso} + Vv_2^{iso}) + (13 + \cos^2 \theta) \frac{Hv}{3} \right\} \sin \theta d\theta \quad (3)$$

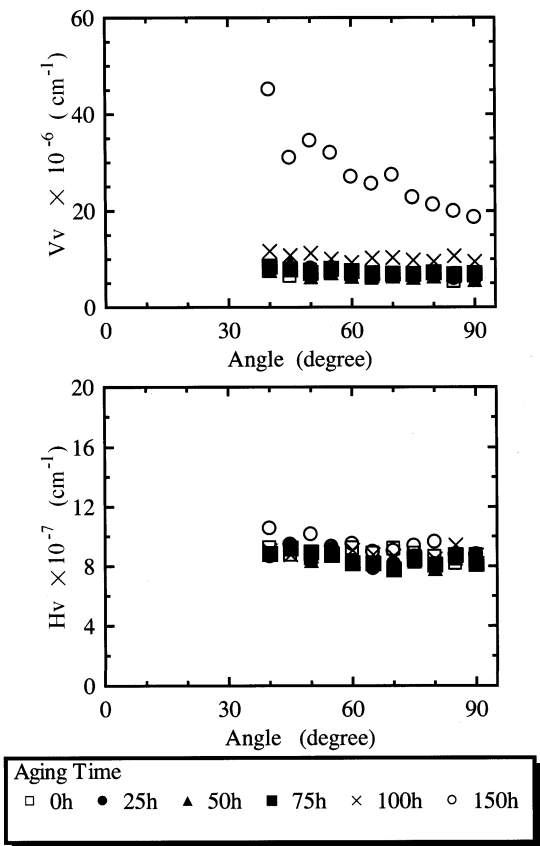


Fig. 4. Scattering loss increment from 12.9 wt.% BEN doped PMMA rod during aging at 70 °C, 95% R.H. at 633- nm wavelength.

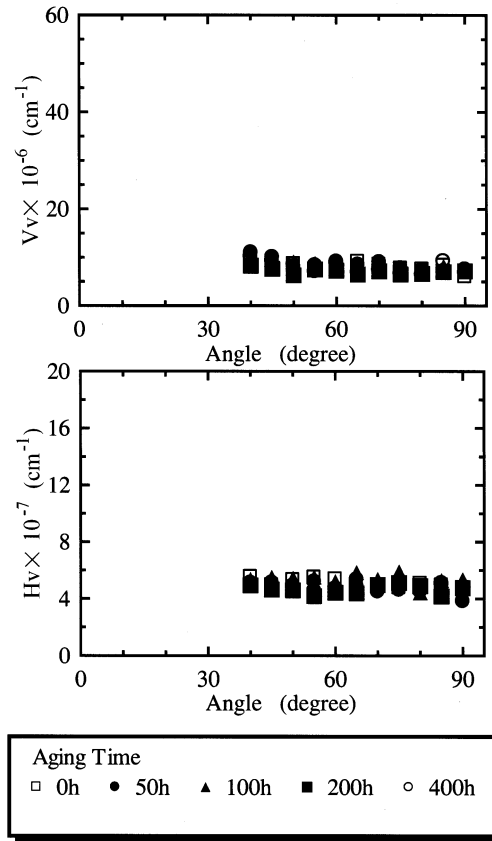


Fig. 5. Scattering loss increment from 9.41 wt.% DPSO doped PMMA rod during aging at 70 °C, 95% R.H. at 633- nm wavelength.

The rearrangement of (10) gives a Debye plot [8], where  $(Vv_2^{iso})^{1/2}$  versus  $s^2$  shows a straight line, and the correlation length  $a$  can be determined by  $a = (\lambda/2\pi)(\text{slope}/\text{intercept})^{1/2}$ .

The  $\alpha_1^{iso}$  term corresponds to the intrinsic scattering loss caused by so-called “thermally induced fluctuations” [8], and is written

$$\alpha_1^{iso} = \left( \frac{80 \log e}{27} \right) \frac{\pi^3}{\lambda_0^4} (n^2 - 1)^2 (n^2 + 2)^2 kT\beta \quad (11)$$

where  $k$  is Boltzmann’s constant,  $T$  the absolute temperature, and  $\beta$  the isothermal compressibility. Since the thermally induced fluctuations may be less than 50 Å in size, which is much smaller than the correlation length  $a$  of the large sized heterogeneities, the  $Vv_1^{iso}$  intensity has no angular dependence. On the other hand,  $\alpha_2^{iso}$  and  $\alpha^{aniso}$  are described as follows:

$$\alpha_2^{iso} = \frac{320 \log e \cdot a^3 \langle \eta^2 \rangle \pi^4}{\lambda_0^4} \times \left[ \frac{(b+2)^2}{b^2(b+1)} - \frac{2(b+2)}{b^3} \ln(b+1) \right] \quad (12)$$

$$b = 4\nu^2 a^2 \quad (13)$$

$$\alpha^{aniso} = \frac{800}{9} \log e \cdot \pi H_V. \quad (14)$$

To clarify the effect of high temperature and high humidity on the scattering loss from the PMMA rod,  $Vv$  and  $Hv$  intensities from the rod before and after aging were measured. Figs. 4 and 5 show the results of PMMA rods doped with benzyl

benzoate (BEN) and diphenyl sulfoxide (DPSO), respectively. Dopant concentrations were chosen to give the same refractive index (1.507) as the core center of the GI POF. The relation between the dopant concentration and the refractive index of doped PMMA was measured for each dopant [11] as shown in Fig. 6, and the appropriate dopant concentration with which the refractive index of 1.507 (index difference  $\Delta n = 0.015$ ) was achieved was adopted for the preparation of PMMA rods doped with these dopants. It is noteworthy that a  $Vv$  scattering intensity increment is observed in BEN doped PMMA after 150 h of aging, while no scattering intensity increase is observed in the DPSO doped PMMA even after 400 h of aging. The change of scattering loss parameter  $\alpha_t$  described by (3) during aging is summarized in Fig. 7 for all kinds of dopant. The scattering loss parameters of BEN, diphenyl sulfide (DPS), and triphenyl phosphate (TPP) doped PMMA rods increased after 100 h of aging, while remarkably no scattering parameter change was observed in DPSO doped PMMA rods even after 1500 h of aging.

It was experimentally observed that this excess scattering loss increment was clearly visualized if the dopant concentration was higher than that shown in Fig. 8. A photograph of a 16.1-wt.% BEN doped PMMA rod after 400 h aging at 70 °C, 95% R.H. is shown in Fig. 8(b) as an example to be compared with the original one before aging in Fig. 8(a). The dopant concentration of 16.1 wt.% was adopted in the case of BEN, with which a high refractive index (1.512,  $\Delta n = 0.020$ ) was obtained. It is

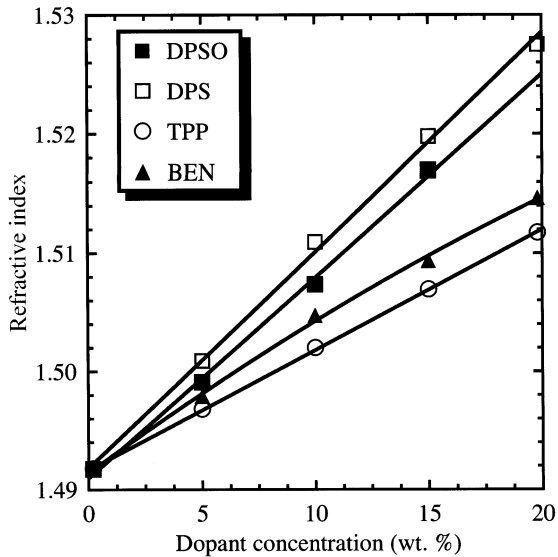


Fig. 6. Relation between the dopant concentration and refractive index of the dopant added PMMA.

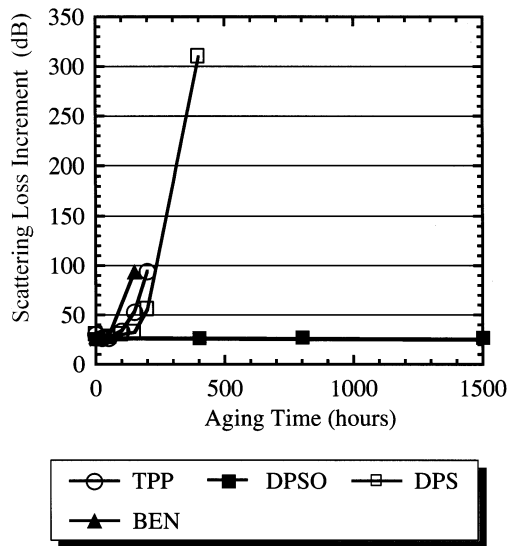


Fig. 7. Change of the scattering loss parameter from the PMMA rods doped with several dopants after aging at 70 °C, 95% R.H. Dopant concentration of each rod was determined to have a refractive index of 1.507.

obvious that the rod became slightly hazy after the aging. Subsequently, this rod was dried in an oven at 70 °C, and the scattering loss change was measured. A photograph of the rod sample after being dried for 100 h is also shown in Fig. 8(c). It is noted that the slightly hazed rod after aging at 70 °C, 95% R.H. became transparent again as shown in Fig. 8(c), and the scattering loss from the rod became almost the same as the original value. The scattering loss parameters  $\alpha_1^{iso}$ ,  $\alpha_2^{iso}$ ,  $\alpha^{aniso}$ , and  $\alpha_t$  are summarized in Table II. It was revealed that the excess scattering loss observed after aging under high temperature and high humidity atmosphere is induced by the water absorbed during aging.

Amount of water absorbed into the PMMA rods doped with BEN, DPS, TPP, and DPSO is summarized in Fig. 9 compared with that of the PMMA homopolymer. Amount of water absorption was estimated by measuring the weight increment of

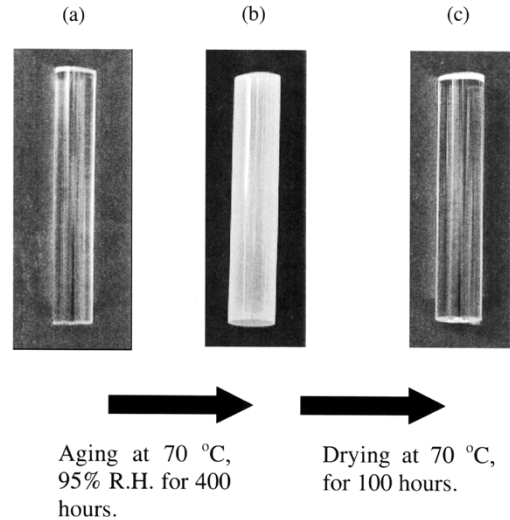


Fig. 8. Photograph of 16.1 wt.% BEN doped PMMA rod after the aging at 70 °C, 95% RH and after drying at 70 °C for 100 h.

TABLE II  
SCATTERING PARAMETER CHANGE OF SLIGHTLY HAZED 16.1 WT.% BEN DOPED PMMA ROD BY WATER ABSORPTION DURING DRYING AT 70 °C

Parameter	Before aging	After 25 h. drying	After 50 h. drying	After 100 h. drying
$\alpha_1^{iso}$ (dB/km)	13.31	11.27	15.02	14.08
$\alpha_2^{iso}$ (dB/km)	1.2	26.48	2.11	1.15
$\alpha^{aniso}$ (dB/km)	13.26	12.83	12.31	12.54
$\alpha_t$ (dB/km)	27.81	50.58	29.44	27.77

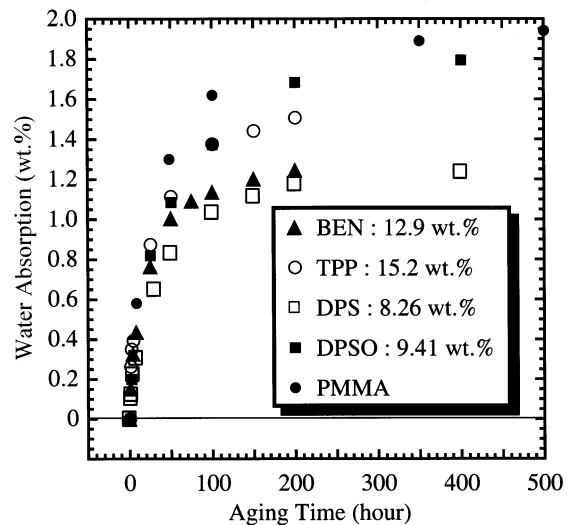


Fig. 9. Amount of water absorption into PMMA homopolymer rod and PMMA rods doped with several types of dopants.

the PMMA rod during aging. The amount of water absorption decreases compared to the PMMA homopolymer when BEN, DPS, and TPP are doped, because those dopants are more hydrophobic than PMMA, whereas almost the same amount of water is absorbed in the PMMA rod doped with DPSO. As

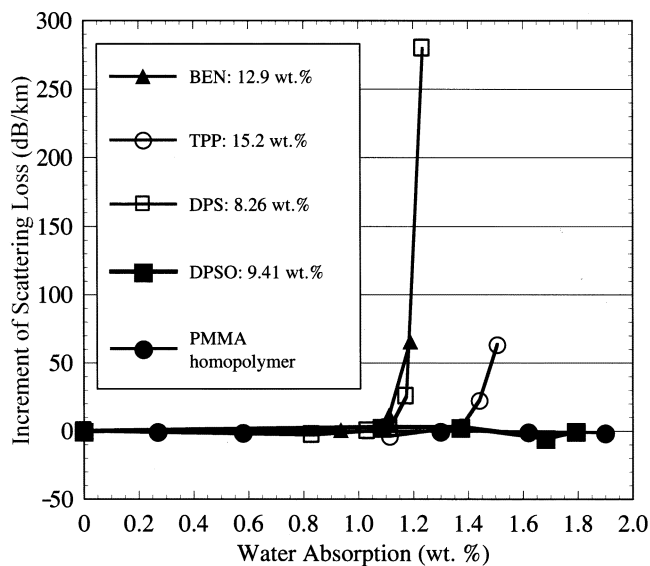


Fig. 10. Relation between the scattering loss increment from the PMMA rods doped with several types of dopants and amount of absorbed water.

shown in Fig. 9, the amount of absorbed water is strongly influenced by the kind of dopant.

The relation between the increment of the scattering loss parameter  $\alpha_t$  from the polymer rod and the amount of absorbed water is shown in Fig. 10 for all kinds of dopant. With increasing the amount of absorbed water, scattering loss also increases. Furthermore, the critical amount of water absorption at which an abrupt increase of excess scattering loss is observed, is dependent on the dopant used. In the case of PMMA rods doped with BEN and DPS, it is noteworthy that a scattering loss increment is observed after aging at 70 °C, 95% R.H. in spite of less water absorption compared to the PMMA homopolymer. Therefore, even if the amount of absorbed water is much smaller in the PMMA rods, this absorbed water cannot be homogeneously dispersed in the polymer but aggregates to form large heterogeneous structures that are thought to induce the scattering loss increment.

A similar scattering loss increment is observed not only from the doped PMMA but also from the copolymer of MMA and benzyl methacrylate (BzMA). The amount of water absorption and scattering loss change of a MMA-co-BzMA rod through the aging at 70°C, 95% R.H. are shown in Figs. 11 and 12, respectively. With increasing fraction of BzMA in the copolymer, the excess scattering after aging becomes higher as indicated in the photograph of Fig. 12. The bottom of the rod became slightly hazy after 24 h of aging in MMA-BzMA (1:1 by weight) copolymer. In the case of the BzMA homopolymer, the increment of scattering loss is visually confirmed and occurs, because the BzMA having an aromatic ring in its monomer unit, is more hydrophobic than PMMA.

In contrast, a PMMA rod doped with 10-wt.% dimethyl sulfoxide (DMSO), which is expected to be more hydrophilic than PMMA was prepared, and its scattering loss change through the aging at 70 °C, 95% R.H. was investigated. The amount of water absorption with respect to the aging time is shown in Fig. 12 in which the photograph of 10-wt.% DMSO doped PMMA rod

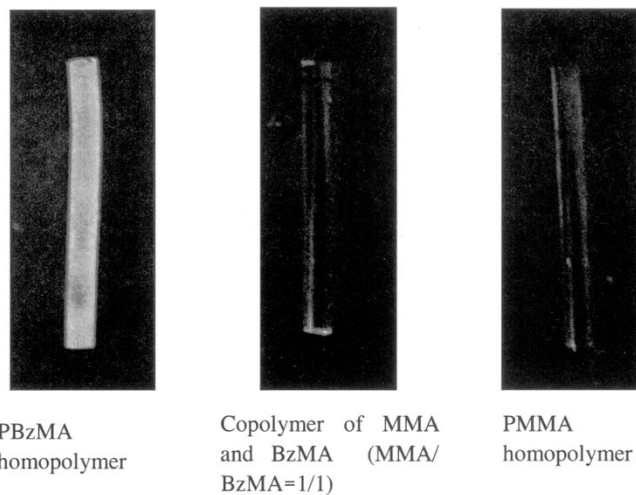
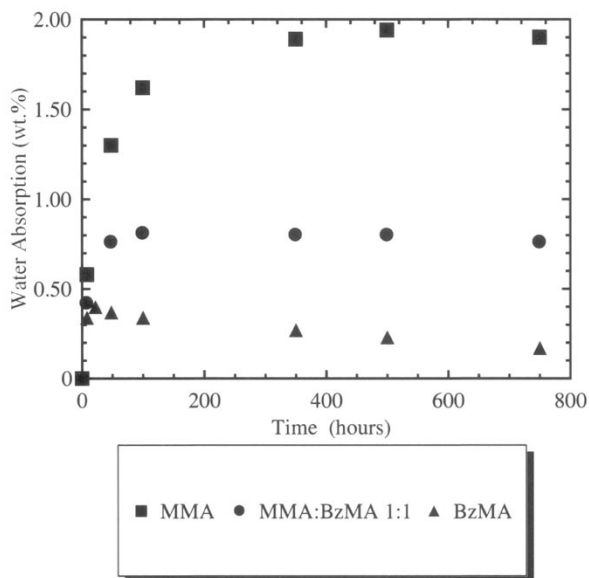


Fig. 11. Amount of water absorption into PMMA, PBzMA homopolymer rods and copolymer of MMA and BzMA rods ( $MMA/BzMA = 1/1$ ) Photographs show the rod samples of PMMA, PBzMA homopolymer, and copolymer of MMA and BzMA ( $MMA/BzMA = 1/1$ ) after aging at 70 °C, 95% R.H. for 24 h.

after aging for 24 h is also shown. Doping with only 10 wt.% of DMSO remarkably increases the amount of water absorption into PMMA. Since more water was absorbed in DMSO doped PMMA compared with the PMMA homopolymer, the excess amount of water molecules, which are no longer uniformly dispersed, aggregated and caused a much higher scattering loss. Consequently, these rods became hazy after only 24 h aging as shown in Fig. 12.

From the results in the above investigations, it can be concluded that selecting an appropriate dopant that is as hydrophilic as PMMA, such as DMSO, should be a key issue for obtaining high humidity stability.

### C. Improvement of Attenuation Stability at High Temperature and High Humidity

From the results of excess scattering loss and water absorption investigations aforementioned, it is clear that the

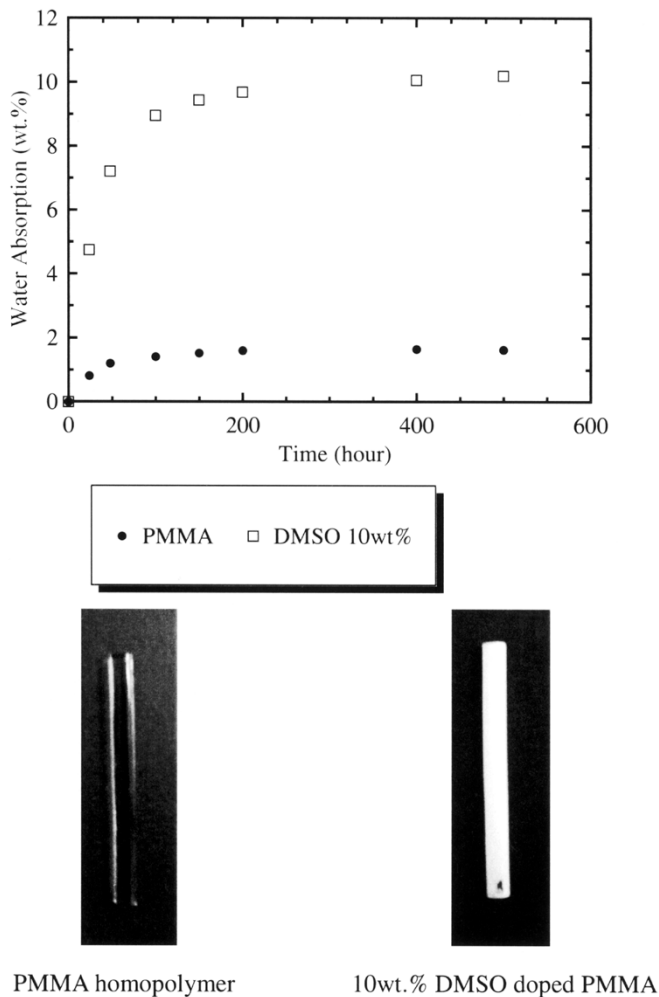


Fig. 12. Amount of water absorption into PMMA homopolymer and 10 wt.% DMSO doped PMMA rods. Photographs show both rods after aging at 70 °C, 95% R.H. for 24 h.

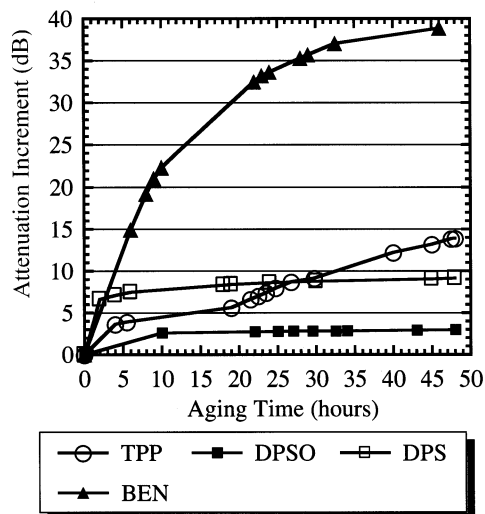


Fig. 13. Attenuation increment of PMMA-dopant system GI POF during aging at 70 °C, 80% R.H. at 650-nm wavelength.

hydrophilicity of the dopant is an important factor for the high humidity resistance of a GI POF. In order to confirm this issue,

the GI POFs doped with BEN, DPS, TPP, and DMSO were experimentally prepared and their attenuation stability at 70 °C, 80% R.H. was evaluated. Since the conditions of 70 °C, 95% R.H. atmosphere under which the fiber should maintain its characteristics are too severe for indoor-use fibers, slightly milder conditions were adopted. The dopant concentration was chosen to obtain the desired numerical aperture (refractive index of core center is 1.507.  $NA = 0.2$ ). During the attenuation stability measurement, both fiber ends were maintained to be connected to the light source and optical power meter, and the attenuation was estimated from the optical power change. The results are summarized in Fig. 13. The attenuation of the BEN doped GI POF significantly increases within only 10 h, while no attenuation increment is observed in the DMSO doped GI POF, which agrees with the results of the excess scattering loss measurement from the doped polymer rod.

#### IV. CONCLUSION

It was shown that high stability in the attenuation at high temperature and high humidity was achieved in the PMMA-dopant system GI POF. It was confirmed that the attenuation increment in the PMMA based GI POF observed when the dopant type and concentration were not optimized, originated in the excess scattering loss induced by heterogeneities formed in the polymer by the aggregation of absorbed water. It was also experimentally confirmed that such an excess scattering increment was eliminated by selecting the suitable dopant having similar hydrophilicity to the polymer matrix. The GI POF obtained using an appropriate dopant had sufficiently high thermal and humidity stability.

#### REFERENCES

- [1] A. K. Dutta and S. Yamazaki, ATM-Forum Document No. 95-0916.
- [2] T. Ishigure, E. Nihei, and Y. Koike, "Graded-index polymer optical fiber for high-speed data communication," *Appl. Opt.*, vol. 33, no. 19, pp. 4261-4266, 1994.
- [3] Y. Koike, T. Ishigure, and E. Nihei, "High-bandwidth graded-index polymer optical fiber," *J. Lightwave Technol.*, no. 13, pp. 1475-1489, July 1995.
- [4] M. Sato, T. Ishigure, and Y. Koike, "Thermally stable high-bandwidth graded-index polymer optical fiber," *J. Lightwave Technol.*, no. 18, pp. 952-968, July 2000.
- [5] M. Sato, M. Hirai, T. Ishigure, and Y. Koike, "Thermal stability of high bandwidth GI POF," in *Proc. Organic Thin Films for Photon. Applicat.*, vol. 18, CA, Sept. 1999, pp. 86-88.
- [6] W. Groh, D. Lupo, and H. Sixl, "Polymer optical fibers and nonlinear optical device principles," *Angew. Chem. Int. Ed. Engl. Adv. Mater.*, vol. 28, no. 11, pp. 1548-1559, 1989.
- [7] M. Sato, M. Hirai, T. Ishigure, and Y. Koike, "Thermally stable high-bandwidth graded-index polymer optical fiber," *J. Lightwave Technol.*, pp. 2139-2145, Dec. 2000.
- [8] Y. Koike, N. Tanio, and Y. Ohtsuka, "Light scattering and heterogeneities in low-loss Poly(methyl methacrylate) glasses," *Macromolecules*, vol. 22, pp. 1367-1373, 1989.
- [9] Y. Koike, S. Matsuoka, and H. E. Bair, "Origin of excess light scattering in Poly(methyl methacrylate) glasses," *Macromolecules*, vol. 25, pp. 4809-4815, 1992.
- [10] P. Debye, H. R. Anderson, and H. Brumberger, "Scattering by an inhomogeneous solid. II. The correlation function and its application," *J. Appl. Phys.*, vol. 28, pp. 679-683, 1957.
- [11] T. Ishigure, M. Sato, E. Nihei, and Y. Koike, "Graded-index polymer optical fiber with high thermal stability of bandwidth," *Japan J. Appl. Phys.*, vol. 37, pp. 3986-3991, 1998.



**Takaaki Ishigure** (M'00) was born in Gifu, Japan, on July 30, 1968. He received the B.S. degree in applied chemistry and the M.S. and Ph.D. degrees in material science from Keio University, Yokohama, Japan, in 1991, 1993, and 1996, respectively.

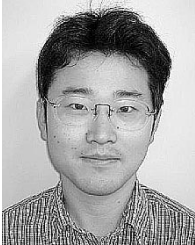
Concurrently, he is an Instructor with Keio University and a group leader of Japan Science and Technology Corporation ERATO "Koike Photonics Polymer Project." His current research interests are in preparation and analysis of a high-bandwidth graded-index polymer optical fiber and its system

design.



**Yasuyuki Tsukimori** was born in Tokyo, Japan, on October 3, 1974. He received the B.S. degree in applied chemistry and the M.S. degree in material science from Keio University, Yokohama, Japan, in 1997 and 1999, respectively.

Currently, he is an Engineer with Asahi-Kasei Corporation, Japan. His current research interest focuses on thermodynamic and optical characteristic analysis of optical polymers.



**Masataka Sato** was born in Akita, Japan, on November 30, 1973. He received the B.S. degree in applied chemistry and the M.S. and Ph.D. degrees in material science from Keio University, Yokohama, Japan, in 1996, 1998, and 2001, respectively.

He has been an Engineer with Fuji Photo Film Company, Ltd. His current research interests are in material science for preparing the high-speed graded-index plastic optical fiber.



**Atsushi Kondo** was born in Kanagawa, Japan, on July 29, 1975. He received the B.S. degree in applied chemistry and the M.S. degree in material science from Keio University, Yokohama, Japan, in 1998 and 2000, respectively. He is currently pursuing the Ph.D. degree from Keio University.

Concurrently, he has been a Researcher with Japan Science and Technology Corporation ERATO "Koike Photonics Polymer Project." His current research interests focus on the optical, temperature, and humidity of photonics polymer.



**Yasuhiro Koike** (M'02) was born in Nagano, Japan, on April 7, 1954. He received the B.S., M.S., and Ph.D. degrees in applied chemistry from Keio University, Yokohama, Japan, in 1977, 1979, and 1982, respectively.

From 1989 to 1990, he was a visiting Researcher at AT&T Bell Laboratories. Since 1997, he has been a Professor with Keio University, where he developed the high-bandwidth graded-index polymer optical fiber. In addition, concurrently, he has been the Director of Japan Science and Technology Corporation ERATO "Koike Photonics Polymer Project" since 2000.

Dr. Koike received the International Engineering and Technology Award of the Society of Plastics Engineers in 1994, and the Fujiwara Award in 2001.